Author Version: *Adv. Oceanogr. Limnol., vol.4(1); 2013; 20-42*

Effects of Iron Availability on Pigment Signature and Biogenic Silica Production in the Coastal Diatom *Chaetoceros Gracilis*

Haimanti Biswas and Debasmita Bandyopadhyaya

National Institute of Oceanography, Regional Center, Council of Scientific and Industrial Research (CSIR), 176 Lawson's Bay Colony, Visakhapatnam 530017, India

Corresponding author: Dr. Haimanti Biswas, 176 Lawson's Bay Colony, 530017 Visakhapatnam, AP, India, email: haimanti.biswas@nio.org, FAX, 0091 891 -2543595

Abstract:

The effects of iron availability on pigment signature and biogenic silica production were investigated for the first time in the coastal diatom *Chaetoceros gracilis* (isolated from the SW coast of Bay of Bengal, India). Results revealed that increase in iron supply considerably increases chlorophyll *a* based specific growth rates, whereas, decreases the values of diatoxanthin index and photoprotective to light harvesting pigment ratios. It is likely that, under iron stress *C. gracilis* activated a strong photoprotection mechanism by maximizing the conversion of diadinoxanthin to diatoxanthin and by increasing over all amount of photoprotective pigments relative to light harvesting pigments. The xanthophyll cycle comprising of diadinoxanthin and diatoxanthin seems to be the principal photoprotective mechanism in *C. gracilis* and is consistent with some earlier studies. This is suggested that under iron limited conditions diatoxanthin index and the ratio of photoprotective to light harvesting pigments can be used as physiological marker for iron stress in *C. gracilis*. The ratios of biogenic silica to chlorophyll *a* were considerably decreased with increasing iron supply indicating the possibility of reduced cellular silica content under iron enriched conditions; however, supplementary information is required to confirm this observation.

Key words: iron, diatom, diatoxanthin, diadinoxanthin, biogenic silica, Bay of Bengal, *Chaetoceros gracilis*, photoprotective, light harvesting, pigments.

1. Introduction:

Many vital physiological processes like respiration, photosynthesis, and nitrogen fixation involve metaloenzymes containing iron (Fe) to facilitate electron transformation [1]. Photosynthesis, the principal physiological process in phytoplankton, requires almost 80% of the total Fe quota for photosynthetic electron transport chains [2]. In absence of sufficient Fe, the rate of carbon fixation can be largely hindered as the absorbed light energy cannot be transferred further due to lack of electron carriers (mainly Fe containing proteins, such as ferredoxin) and the surplus energy can potentially form reactive oxygen species leading to photodamage of the cell [3]. Dissolved Fe has extremely low solubility in the marine environment. In some major high nutrient low chlorophyll (HNLC) regions of the global ocean, Fe has been found to control phytoplankton primary production [4].

Diatoms are one of the major contributors not only in marine primary production, but also to global primary production and are famous for their ubiquitous distribution in the contemporary oceans [5]. Several in situ Fe fertilization experiments have been conducted in the past in order to enhance the rate of primary production in those HNLC oceanic areas and it has been observed that diatoms were the most successful phytoplankton group in all Fe induced blooms [4]. However, the physiological responses of marine diatoms to Fe stress might be useful tool to denote inadequacy of Fe in the ambient waters. Many studies have been conducted till yet to find out an appropriate physiological marker indicating Fe stress in phytoplankton. Fe starved marine diatoms have been observed to show a significant reduction in Fe containing proteins synthesis [6] and functionally equivalent replacement with non Fe containing proteins. For example, replacement of ferredoxin by flavodoxin [3] and flavdoxin has widely been used as a physiological marker to examine Fe stress in marine phytoplankton [7, 8, 9]. Marine diatoms show high variability in pigment signature [10] and biogenic silica production [11] in response to Fe stresses and in this study we have tried to examine if these variability can be used as a physiological marker for Fe stress for a particular diatom species.

In general, under high light and low Fe, diatoms protect their cells from photodamage by altering the biosynthesis of different carotenoids which can be reflected in their pigment signature [12]. Diatoms have been observed to down-regulate their light harvesting capacity coupled with up-regulated photoprotection mechanism in response to Fe stress which can be evidenced in the ratios between the total pool of photoprotective (PP) to light harvesting pigments (LH). Hence, an increased value of

photo-protective (PP) carotenoids to light harvesting (LH) pigments could be indicative of Fe and light stress [13] in marine diatoms.

It has been well documented in diatoms that under light stress, the xanthophyll cycle dissipate excess absorbed light energy by enzymatic conversion between epoxy-containing xanthophyll pigment and epoxy-free xanthophylls [14]. The major xanthophyll cycle pigments of diatoms are diadinoxanthin (DD) and diatoxanthin (DT) comprise the diadinoxanthin cycle (DD-cycle), whereas, some diatoms may also possess the Violaxanthin cycle [15]. Under light/Fe stress the xanthophyll cycle in diatoms activates the forward conversion of DD to DT which is a short-term photoprotective mechanism [16, 17]. Therefore, the relative changes in DD and DT provide the information about Fe and light stress over a short time scale. presence of higher amount of DT over DD usually represent the phenomenon of non-photo-chemical quenching where light energy is being dissipated as heat energy by an enzymatic de-epoxidation process [10]. As a result, DT index (DT/[DT+DD]) can be used as an indicator of Fe/Light stress in diatoms. it should be noted that, although, β-carotene takes active part in the process of photoprotection in some algal groups like green algae, in Fe/light stressed diatoms DD concentrations have been observed to be higher compared to β-carotene leading to the ratios of DD to β-carotene greater than one [10, 18].

Fe starved diatoms have been observed to form heavily silicified cells, whereas, Fe enriched cells form thinner frustules [19, 20, 11] when nutrients are replete. However, exceptions have also been reported in some diatom species where cellular silica content did not show any variation in response to Fe level [21]. The underlying mechanisms for such observations have been explained by different authors and were found to be related to nitrate/silicate uptake rates, delay in cell division process and change in surface area to volume ratios of siliceous frustules in response to different Fe concentrations [22, 23, 24]. A decrease in BSi:Chl *a* ratio in Fe enriched cells could also result from faster increase in Chl *a* concentrations compared to BSi production in response to Fe enrichment. Hence upon the supply of Fe, diatoms show a shift from higher BSi:Chl *a* ratios to low BSi:Chl *a* ratios and can be used as an indicator of Fe availability.

Although, coastal waters are believed to not be Fe limited and the dissolved Fe levels may experience wide fluctuations daily, weekly, monthly and seasonally. However, our knowledge is meager about the fact that if Fe concentrations may affect the pigment signature, photoprotective mechanism or

biogenic silica production in diatoms from the study area. Virtually, no study has been done on any isolated diatom species or natural assemblage showing the variability in pigment signature in response to different Fe concentrations from this region. The present study has been undertaken to understand the variability in pigment signature and biogenic silica production in the coastal diatom *C. gracilis* under different Fe concentrations and its possible use as a physiological marker to detect Fe stress in the coastal waters.

2. Materials and Methods:

2.1 Study area

The study area, Visakhapatnam coast is a coastal embayment (Fig. 1) in the SW coast of Bay of Bengal (17º44´N and 83º23´E) and the coastal waters receives large input of freshwater discharge during Indian summer monsoon leading to low salinity, higher turbidity and lower light penetration [25]. However, the scenario can be completely opposite during the dry periods and this large variability may lead to a wide fluctuations in the dissolved Fe level as well as light availability in the coastal waters. In order to adjust to such variable light and Fe availability, it is presumed that the dominant coastal diatom species may possess a strong photo-protective mechanism which can be dependent on Fe availability. Different species of *Chaetoceros* and *Skeletonema* [26] were observed to be the most abundant diatom groups in the entire coast throughout the year. As a result, for our study we have chosen *Chaetoceros gracili*s, which typically blooms in response to nutrient enrichment.

2.2 Pre-culture:

Chaetoceros gracilis a common coastal diatom was isolated from the coastal water of Visakhapatnam (17°42′108″N and 83°19′064″E) (Oct 2011) (Fig. 1), and was grown in 0.2µm sterile filtered seawater (also collected from the coast) enriched with standard addition of nitrate (200µM NO_3), silicate (100µM SiO_3^{-2}) and phosphate (15µM PO_4^{-3}). Unlike other metal incubation experiments [27] the culture media was not completely metal free. The filtered coastal water was kept absolutely natural without adding any other growth promoting agents except the addition of the major nutrients (N, P, Si) as stated above. Diatom cells were grown inside 1L polycarbonate bottles from Nalgene, USA. Prior to utilization, all bottles used for growing diatoms were washed with 10% HCl followed by milli-Q water (MQ) repeatedly and kept inside zipped lock plastic bags till utilized. The cultures were usually

diluted to a Chl *a* concentration of ≈ 1µg L^{-1} on every third day from the last dilution and allowed to grow till the chlorophyll concentration reached 10-15µg L^{-1}. The semi-continuous cultures were grown in polycarbonate bottle kept inside a water bath placed under natural day and night period (in Nov the actual day and light cycle in the study area is 12:12 hrs cycle). Light intensity during the growth of the pre-culture was measured using a digital lux meter (METRAVI 1330, METRAVI, WB, India) fitted with a silicon photodiode with filter. Light intensity was recorded in every hour from 6hrs to 17hrs and it varied from 1.4 -1142µmol m^{-2} s^{-1} (Fig. 2a). The water temperature was recorded with a mercury thermometer and it varied from 24-28 °C (natural variation without any temperature control).

2.3 Experimental setup:

Coastal waters (17°42′108″N and 83°19′064″E) were usually collected with the help of a motor driven boat using pre-cleaned Niskin sampler and carried to the laboratory inside the 20L acid cleaned polycarbonate carboys (Nalgene). These water samples were first filtered with GF/F filters (to remove all particulate biomass) followed by another filtration using 0.2µm polycarbonate filters (to remove bacterial biomass). Initial nutrient levels were measured and final nutrient levels were adjusted to the level as mentioned above. The diatom cultures were incubated under a wide range of Fe concentrations (25 -2000nM) with a total of 20 Fe levels. In addition to these, one control was also kept without addition of any Fe. It must be noted that the control in our experiment cannot be considered as "zero metal" but expected to have the natural metal concentration existing in the sampling area. Fe concentrations were not measured in the background water during the experimental period. The available literature showed that the total dissolved concentration of Fe was previously estimated to be 54.28±1.38nM in the study area [28, 29]. However, the total dissolved Fe concentration does not represent the bioavailable fraction and only a small fraction of the total dissolved metal pool might be present in inorganically complexed form or as free hydrated form. Almost 80-99% of the dissolved Fe can be present forming strong complexes with organic binding ligands mostly of biological origin [30]. We thus assumed that even if > 90% of the dissolved Fe present in the study area was organically chelated; the rest 10% of the total dissolved metal could be bioavailable and accordingly we have calculated the probable bioavailable fraction from the concentrations obtained from the previous studies (54.28nM Fe) which revealed that 5.43nM can be present as bioavailable fraction in the study area. But there might be significant deviations from this value in different time scales (daily, monthly, and

seasonal). However, for our experiments the selected iron concentrations were always higher than 5nM. The added Fe was chelated with Ethylenediaminetetraacetic acid (EDTA). The analytical grade of $FeCl_3$, $6H_2O$ and EDTA disodium salt were procured from the Merck chemicals (Germany) and the solution was prepared in 1:5 ratio and added according to the required volume in order to reach the target concentrations.

Once the bottles were ready with the target concentration of Fe, 1-5ml of the pre-cultures were taken from the exponential growth phase (mostly after 48 hours) and added to each experimental bottle to get the final concentration of Chl a ≈ 1µg L^{-1}. The bottles were mixed gently and were transported to an outdoor incubator. The entire procedure was performed in a clean room with extreme care to avoid any kind of contamination of other metals. The incubated cultures were grown under the sun (the average light intensity is given in Fig. 2a) keeping inside a water bath (for availing natural day-night cycle and temperature). Every day the bottles were mixed very gently with care at a particular time to avoid any sedimentation of biomass at the bottom of the bottles. During the pre-culture phase, a separate monitoring was done to understand the growth pattern of the culture grown under nutrient replete conditions. Usually, the highest growth rates were observed within 48 -62 hours. Hence, during the experiment, every sampling was done on the 3rd day after the incubation. All bottles were brought back to the clean laboratory for further sampling and analysis.

2.4 Sample Analysis:

One hundred ml samples were filtered from each treatment using GF/F filter for total Chl a estimation and were kept at -20ºC until analysis. Later, the filters were soaked overnight in 5ml DMF (N,N-Dimethyl formamide) following the methodology of Suzuki and Ishimaru [31] and the fluorescence was measured using a fluorescence spectrophotometer from Varian (Carry Eclipse). Chl a based specific growth rates were calculated as follows:

$\mu = (t_2 - t_1)^{-1}. \ln (N_2/N_1)$ where, μ is the net growth rate d^{-1} and N_1 and N_2 are the Chl a concentrations at t_1 and t_2, respectively.

For analyzing Biogenic silica 100 ml aliquots were collected and filtered using 0.2µm polycarbonate filters (GTTP from Millipore). The filters were washed with 0.2µm filtered seawater, folded in quarter and kept inside individual plastic petri dishes and oven dried in 60ºC overnight.

Thereafter the filters were digested in 0.2N NaOH inside a water bath (80°C) for 5-6 hours. 0.2N HCl was added to neutralize the sample and one aliquot of this solution (preferably 1ml) was taken and diluted to 25 ml [32]. Silicate concentration was measured using the colorimetric methodology of Strickland and Parsons [33]. A blank filter was also digested and treated in the similar way as samples to measure the reagent blank.

A HPLC from Agilent Technology (Series 1200) was used to quantify the pigments following the method proposed by Heukelem and Thomas [34] against the standard pigments procured from Sigma Aldrich (USA) and DHI (Denmark). The method is based on a reverse phase chromatographic technique which employs a polar aqueous mobile phase and the hydrophobic molecules in the polar mobile phase tend to adsorb to the hydrophobic stationary phase. But the hydrophilic molecules in the mobile phase will pass through the column and are eluted first. We used C8 HPLC column (ZORBAX eclipse XDB-C8, 4.6mm (diameter) x150 mm (length); pore size 3.5µm; PN: 963967-906). A methanol-based reversed-phase gradient solvent system and a simple linear gradient (binary gradient elution using solvent A: 70 : 30 methanol : 28mM Tetra Butyl Ammonium Acetate (TBAA) at pH 6.5, solvent B: methanol; Linear gradient from 5–95% solvent B in 22 min, isocratic hold, of 95% solvent B) were applied. The column temperature was kept at 60◦C.

For HPLC pigment analysis, 25-50ml water samples were filtered on 25 mm GF/F filters using a vacuum pump (Rocker 600 from Tarsons, India) keeping the pressure 200mb. The filtration was done under low light to avoid any photo degradation of pigments. Immediately after the filtration the filters were folded and wrapped inside individual pieces aluminum foil and kept at -20ºC until analysis. The extraction was performed later by soaking the filters overnight in 3-5ml 90% acetone (HPLC grade from Merck chemicals) keeping inside an amber color bottle and was kept at -20°C to prevent photo damage. A tissue homogenizer (Ultra Turrax, Germany) was used to break the cells keeping the bottles on an ice filled tray followed by cold centrifugation at -10°C (Eppendorf, Germany). The supernatant was taken and mixed manually with a buffer composed of 28 mM aqueous TBAA (AR Grade, Fluka) at pH 6.5 and methanol (GC Assay 99.7% pure, Merck) in 90:10 ratios. The injection volume was 400µl. The column pressure was kept at 200b (maximum) with a solvent flow rate of 1.1 ml min^{-1}.

3. Results:

C. gracilis showed significant responses to increasing Fe levels. Growth rates, BSi production and pigment signature of *C. gracilis* were found to be highly sensitive to Fe availability. The experiment was repeated four times considering different Fe levels. Fluorometric analysis of total Chl *a* was done for all experiments, whereas, BSi production wasn't measured for the second set of experiment and are given in Table 1. HPLC pigment analysis was done for the first and the fourth experiment and different pigment ratios have been presented in Table 2. Linear regression analysis was done for each parameter in relation to different Fe level over the experimental range and the results given in Table 3. Paired t-test was performed between the control treatments and Fe enriched samples for some parameters to show the statistical significances in the observed differences and the results are presented in Table 4.

3.1 Chl *a* production and growth rate:

Chl *a* concentrations measured by fluorometric analysis are presented in Table 1 and Fig. 2b. A significant enhancement in Chl *a* concentration was observed in relation to Fe addition. Chl *a* concentrations (Fig. 2b) showed logarithmic trend in response to increasing Fe concentrations with a significant R^2 value ($R^2 = 0.724$, n =35, $P < 0.001$). In the untreated controls, the average concentration of Chl *a* was 7.06±0.9µg L^{-1} (Table 1) which was found to be 1.88 times higher following addition of 25nM Fe. The degree of enhancement in Chl *a* concentration was almost 17 times higher at 200nM Fe treatment compared to the control. The corresponding % increase in the growth rate was 121% within the Fe concentration range of 80 -1000nM compared to the untreated control (Fig. 2c). After 200nM Fe concentration, Chl *a* concentrations were found to reach a plateau and remained almost constant with little variation till 2000nM Fe concentrations. Two sample t-test was performed using Chl *a* concentrations from 1) all control treatments and 2) Fe treated samples (25-2000nM) and the observed t-value revealed that the difference between these two sets are statistically significant (Table 4; t = -42.6, n =33, P<0.001).

3.2 Pigment composition:

HPLC pigment analysis revealed that beside the presence of Chl *a* in the cell extracts of the diatom *Chaetoceros gracilis,* considerable amount of fucoxanthin (Fuco), diatoxanthin (DT), diadinoxanthin (DD), chlorophyll *c* (Chl *c*) and *β*-carotene were also present in all samples with variable amounts. The chromatograms (from control, 25, 50, 100, 150 and 500nM Fe treatments) from the reverse phase HPLC for the pigment mixtures from the forth experiment are presented in Fig. 3. All

pigments were found to increase linearly from the control to 150nM Fe level and then reached more or less a constant value till 1000nM Fe level (Fig. 4a, 4b and Fig. 5a, 5b, 5c). Chl *a* concentrations measured by HPLC and fluorometric method were highly linear and showed a significant positive correlation ($R^2 = 0.917$, n =16, P <0.001) (Fig. not shown here). The concentrations of Fuco and Chl *c* were increased in parallel with Chl *a* revealing high R^2 values with increasing Fe concentrations (Table 3; Fig. 4a and 4b). Ratios of all pigments to Chl *a* from both experiments have been given in Table 2. The ratios of Fuco/Chl *a* were almost constant (0.37±0.015) irrespective of Fe concentrations. No significant changes ($R^2 = 0.006$, n =15, p > 0.1, Table 3) in the ratios of Chl *c* to Chl *a* were observed with increasing Fe concentrations (Fig. 4d). The average values of Chl *c* to Chl *a* ratios from the control treatments and 200nM Fe treatments were eaxactly similar (0.078±0.013) (Table 2) indicating that although the concentrations of these pigments were enhanced, the magnitude of enhancement was constant in response to increasing Fe supply. This observation was further supported by the ratios of Fuco/Chl *c* in relation to different Fe levels (Fig. 4e) (R^2 =0.123, n =15, p>0.1, Table 3). Two sample t-test showed that fuco: Chl *a* and Chl *c*: Chl *a* ratios derived from the controls and Fe treated samples did not reveal any statistically significant difference (Table 4).

The concentrations of DD (Fig. 5a) and *β*-carotene (Fig. 5c) were enhanced significantly (Table 3) with increasing Fe levels, but DT concentrations (Fig. 5b) depicted an insignificant trend. Interestingly, the ratios of DD to Chl *a* (Fig. 5d) and *β*-carotene to Chl *a* (Fig. 5f) revealed insignificant correlations with increasing Fe concentrations (Table 3). However, the average values of *β*-carotene to Chl *a* ratios observed in the untreated controls was 0.079±0.001, whereas, almost 18% enhanced values were noticed in all Fe enriched samples (Table 2). Interestingly, this ratio remained almost similar within different Fe concentrations. Paired t-test revealed that the difference was statistically significant (Table 4). The ratios of DT to Chl *a* (Fig. 5e) showed an exponential decrease with respect to Fe concentrations. This ratio was decreased by almost 82% in the 200nM Fe treatments compared to the control treatments (Table 2). The highest values of DT to Chl *a* ratio were observed in the untreated controls and 25nM Fe treatment suggesting that DT synthesis was maximized under low Fe concentrations.

Fig. 6a depicts DT index [DT/(DT+DD)] in relation to different Fe concentrations. DT indexes were found to be decreased exponentially with increasing Fe concentrations and was statistically

significant (R^2 = 0.854, n =15, p < 0.001). Two sample t-test revealed that the difference between DT index derived from the controls and Fe treated samples were statistically significant (t = 8.1, DF = 13, p < 0.001). Fig. 6b represents the ratios of DD to β-carotene and was found to decrease with increasing Fe concentrations (R^2 = 0.609, n =15, p > 0.05). In cells grown in the untreated control the ratio of DD to β-carotene was found to be ≈ 35% higher compared to the ratios observed in the Fe treated cells (Fig. 6b). t-test values also revealed that the difference between the ratios derived from the control and Fe treated cells were statistically significant (Table 4).

The concentrations of Chl *a*, Fuco, Chl *c* from different Fe treatments were added together to get a total concentration of the Light Harvesting pigments (LH). Similarly, the sum of DT, DD and β-carotene were considered as photoprotective pigments (PP). Fig. 7a and 7b represent the total concentration of LH and PP pigments in relation to different Fe concentrations. The results clearly show that there were significant increases in both LH and PP pigments with increasing Fe concentration (R^2 = 0.848 and 0.788; n = 15; p <0.01). However, a significant decrease was observed in PP/LH pigment ratios with increasing Fe concentrations (Fig. 7c) (R^2 = 0.766, n = 15, p < 0.001). This indicates down regulation in the synthesis of PP pigments relative to LH pigments with enhanced Fe addition. The maximum value (0.31±0.015) of PP/LH pigments was observed in the untreated controls and decreased 38% in the 200nM Fe treatment (Table 1). This result clearly indicates that this diatom species down regulated the synthesis of photoprotective pigments under iron enriched condition and maximized the synthesis of the same when Fe was limited. Two sample t-test value proved that the difference between PP/LH ratios of controls and Fe treated samples are statistically significant (t = 9.37, DF =13, P < 0.001) (Table 4).

3.3 Biogenic silica production and silicate uptake:

Compared to Chl *a*, total particulate biogenic silica production also showed a similar trend to increasing Fe levels (Table 1, Fig 8a). The minimum value (7.90±0.93µM) of biogenic silica content was observed in the control treatments and a linear increase was observed from the 25nM Fe treatment (8.21±1.27µM) to 200nM Fe treatment (45.47±8.10µM) and reaching a plateau thereafter till 1000nM Fe concentration. A significant positive correlation was observed between Chl *a* concentrations and biogenic silica contents (R^2 =0.758, p < 0.001, n =18) (Fig. 8b). Surprisingly, the ratios of BSi to Chl *a* revealed an opposite trend (Fig. 8c) and revealed a significant decrease with increasing Fe

concentrations (Table 3). The maximum value of biogenic silica to Chl *a* was determined in the untreated controls (1.32±0.33µmol µg $^{-1}$) and it was decreased 47.5% in the 25nM Fe level followed by further 55.4% and 72% drop down in 50 and 200nM Fe levels, respectively. Two sample t-test was performed between BSi:Chl *a* ratios from the controls and Fe treated cells and it revealed that the difference between these two sets of data was statistically significant (Table 4). BSi:Fuco ratios were also plotted against increasing Fe levels (data not shown here) and a significant decreasing trend was observed (R^2 = 0.779, n =15, P< 0.001).

The final concentrations of silicate were measured from the last two experiments and the net amounts of silicate (Initial –final) consumed during the experimental phase have been given in Table 1. There was a concomitant decrease in the final silicate concentrations with increasing growth rate and the net silicate uptake values revealed a significant positive correlation (R^2 =0.951, n =18, P <0.001) with the BSi contents from different Fe treatments.

4. Discussion:

4.1 Chl *a* production and growth rate:

The significant increase in Chl *a* concentrations and growth rates (Fig. 2a, Table 1) in response to increasing Fe supply clearly indicates that Fe availability considerably affects Chl *a* synthesis in *C. gracilis*. Our observations are in agreement with earlier studies where a significant enhancement in Chl *a* synthesis was observed in different diatom species when supplied with Fe [10]. A decline in chlorophyll content in response to Fe stress has been reported in eukaryotic algae [6] and also in cyanobacteria [35]. Fe controls the process of chlorophyll synthesis directly and indirectly and Fe stress induces chlorotic cells in diatom [36]. There are several Fe containing metaloenzymes involved in the process of chlorophyll synthesis. For example, Fe containing coproporphyrinogen oxidase catalyses the conversion of Mg protoporphyrin to protochlorophyllide [37]. Chlorophyll precursor δ-aminoleuvulinic acid synthesis is also Fe dependent [38].

However, Fe limitations can also indirectly affect the process of chlorophyll synthesis by controlling the process of nitrogen metabolism. Nitrogen is essential to build the porphyrin ring of chlorophyll molecule [8] and the major enzymes involved in nitrate and nitrite metabolism are Fe containing proteins and as a result, under high nitrate but low Fe conditions, Chl *a* synthesis in diatoms

can largely be hampered [39]. There are many oceanic areas where despite of high nitrate, phytoplankton productivity is quite low. Scientific investigations revealed that due to inadequacy of Fe, phytoplankton were unable to metabolize the available nitrate efficiently in those systems. Interestingly, massive diatom blooms were always observed in all in situ Fe fertilization experiments conducted in the HNLC regions of the global oceans [40, 4]. This indicates that diatoms must possess some specialized mechanisms to bloom easily in response to Fe enrichment. Recently, Marchettii et al. [41] conducted a detailed study based on metatranscriptomics to determine the molecular basis for the physiological responses of marine phytoplankton to Fe stress. This study revealed that under Fe-replete conditions the genes involved in nitrogen metabolism were well expressed indicating that diatoms can efficiently allocate the newly acquired Fe to nitrogen metabolism which makes them the most successful phytoplankton group in all Fe induced blooms in different oceanic areas. During the present experiment, although *C. gracilis* was grown in nitrate enriched seawater, it is likely that the amount of Fe present in the untreated controls was insufficient for metabolizing the given nitrate and Chl *a* synthesis.

Fe stress may also control chlorophyll synthesis by affecting the process of protein synthesis in plant cells. Usually, the pigment cannot remain alone inside the cell as it is toxic, but rather, only in the presence of the appropriate protein can the cellular pigments be accumulated as pigment protein complexes [42]. Protein synthesis is a genetically controlled mechanism where the redox state of the electron transporting protein (e.g. cytochrome b6/f or plastoquinone) is responsible and controls the transcriptional process of protein synthesis [43]. Thus, in Fe limited cells, the process of protein synthesis also affects the chlorophyll content of the cell as Chl *a* alone cannot function in the absence of the chlorophyll binding proteins [44]. In the present experiment, protein synthesis might have been hindered in the untreated controls by Fe limitation, hence exhibited slow growth rates and low chlorophyll values. Upon the supply of Fe, nitrogen metabolism followed by protein synthesis was probably up-regulated resulting in higher growth rates and Chl *a* synthesis.

4.2 Pigment composition:

C. gracilis showed considerable variability in pigment signature in response to different Fe concentrations. Notable differences in pigment composition in response to Fe availability have been reported in many marine and coastal diatom species [45, 46, 6, 10, 47] and our observations are consistent with existing literatures. The unaltered ratios of Fuco/Chl *a* and Chl *c*/Chl *a* (accessory light

harvesting pigments) to increasing Fe supply clearly indicates that these pigments did not take part in the process of photoprotection. Kashino and Kudoh [48] also demonstrated that *C. gracilis* (Schuett) showed no variation in the ratios of Fuco, Chl *c* and *β*-carotene to Chl *a* when exposed to different light conditions. HPLC pigment analysis clearly indicated that the coastal diatom species possess a strong photo-protective system when exposed to low Fe and high light conditions (during the present experiment the photon flux density varied between 1.4 -1142µmol m^{-2} s^{-1} (Fig. 2a). Under light sufficient conditions, phytoplankton continuously absorb photons which must be transferred through Fe containing electron carriers for carbon dioxide fixation via Calvin cycle [2]. In absence of sufficient electron carriers, excess energy can get accumulated inside the cell generating reactive oxygen species which may potentially cause photodamage to the cell [11]. In order to protect the cell from such potential damage, some physiological processes must be implemented and usually photoprotective carotenoids (it may largely vary according to the algal class) fulfill this vital job in protecting the cells [49]. Thus, under low Fe/high light conditions, more photoprotective (PP) carotenoids are synthesized over light harvesting (LH) carotenoids in order to minimize the quantity of light capture and photodamage. Our results clearly depicted that maximum value of PP/LH pigment ratio (Fig. 7c, Table 2) were noticed in the untreated controls indicating Fe limitation.

Khasino and Kudoh [48] identified DD cycle as the main photoprotection mechanism in *C. gracilis* Schuett (a temperate strain) and the authors showed significant variations in DD and DT pool in response to different light exposures. Similar trend was observed in the present study where both DD and DT showed considerable variations in response Fe supply. The major phytoplankton groups in the coastal and marine environment including diatoms, dinophytes and haptophytes possess a xanthophyll cycle where they can convert DD to DT (by a single de-epoxidation step) by non-photochemical quenching to dissipate surplus absorbed light energy [50]. DT index [(DT)/(DT+DD)] represents the occurrence and magnitude of non-photochemical quenching in these groups of phytoplankton. In the present experiment, the highest values of DT index (Fig. 6a, Table 2) were observed in the untreated controls indicating that *C. gracilis* maximized the conversion of DD to DT probably because of inadequate Fe supply. DT index was decreased by 64% in the 200nM Fe level depicting reduced conversion of DT to DD with Fe addition. This observation confirms the fact that under the given light condition, the available Fe in the ambient waters was insufficient to utilize the absorbed light energy, hence enhanced the photoprotection mechanism by maximizing DT index and PP/LH pigment ratios. A

similar result has been described by Juhas and Buechel [51] in a marine diatom *Cyclotella meneghiniana*, where under high light and low Fe, higher values of DT/DD was observed. Laviale and Neveux [18] conducted a study by exposing 11 different marine phytoplankton species including a diatom, *Skeletonema costatum* to a range of light intensities from 10 -700μmol m^{-2} s^{-1} and the cultures were grown in F/2 medium where Fe concentration is quite high (in the μM level). The ratios of DD/Chl *a* were increased with increasing light intensities, however, DT was only observed when cells were exposed to 700 μmol m^{-2} s^{-1} l photon flux density and the ratio of DT/Chl *a* was 0.045. For the present experiment, the average light intensity was 650 μmol m^{-2} s^{-1} and the average value of DT/Chl *a* ratio was 0.05 for all Fe enriched samples. This observation clearly demonstrates that marine diatoms may tolerate high level of irradiance when Fe is sufficient, but after a certain light intensity, photoprotection system gets turned on despite presence of Fe.

It should be noted that the ratio of DD to Chl *a* was not decreased significantly as observed in the case of DT in response to Fe enrichment. This indicates that under Fe enriched condition, the need of non-photo-chemical quenching was minimized, although DD was produced. According to Goericke and Welschmeyer [52], DD also can act as a precursor for Fuco. Kashino and Kudoh [48] observed that when some dark adapted cells of *C. gracilis* (Schuett) were exposed to high light, DD cycle pigment pool size was significantly increased and remained high even after cells were brought back to dark. The concentrations of DD were always higher than *β*-carotene (all values were > 1) indicating more DD production than *β*-carotene. A similar observation was reported in the marine diatom *Phaeodactylum tricornutum* [10].

Although, *β*-carotene is a well known antioxidant, however, may also act a precursor of other carotenoids like DD and Fuco. It has been shown that in some marine diatoms, both DD and Fuco are synthesized from *β*-carotene via violaxanthin [49, 12]. Fujiki and Taguchi [53] observed a constant *β*-carotene to chlorophyll ratio (0.05) irrespective of different light intensities in three different diatom species including *C. gracilis*. Kashino and Kudoh [46] reported a similar trend in *C. gracilis*. In the present study this ratio was found to be almost 18% higher in the Fe treated samples relative to the controls. The study by Kosakowska et al. [10] also reported a similar result where the average values of DD/*β*-carotene were increased by almost 55% when Fe level was increased from 10 to 100nM. In the

present study, the observed increase in β-carotene concentrations in response to increasing Fe level (Fig. 5c) could be because of the fact total pool of β-carotene was increased as a precursor of other pigments.

Different species of *Chaetoceros* have been studied by many authors and reported similar responses to Fe and light stress from various parts of the global ocean [54, 47, 55]. In a study by Dimier et al. [56], it was observed that among three diatom species (*Skeletonema marinoi, Thalassiosira rotula and Chaetoceros socialis*), *Chaetoceros socialis* showed maximum photo-adaptability which was thought to be the key reason for the formation of spring blooms by this species in some coastal areas. In the present study, *C. gracilis* was isolated from the coastal waters, where wind induced mixing necessitates that diatom species must possess a strong photo-adaptability presumably by activating their xanthophyll cycle.

4.3 Biogenic silica production and silicate uptake:

Iron limited diatoms often show increased cellular silica contents indicating that diatoms grow thicker under Fe limited conditions [11]. In the present study, occurrences of Fe limitation in the untreated controls were well evidenced in the pigment signature (DT index and PP/LH pigment ratio) of *C. gracilis*. Our observations suggest that Fe replete cells of *C. gracilis* exhibited lower biogenic silica per unit Chl *a*, whereas, cells grown in the untreated controls show almost 47.5 -72% higher BSi:Chl *a* ratios. It is likely that, *C. gracilis* cells in the untreated controls produced more silicified cells coupled with low Chl *a* contents resulting in high BSi:Chl *a* ratios. The values of net silicate uptake also showed a similar pattern supporting the fact. Whereas, after Fe addition, enhanced chlorophyll synthesis and reduced silicification resulted in decreased BSi:Chl *a* ratios. This observation is in agreement with existing literatures. Hutchins and Bruland [19] reported the occurrence high BSi:Chl *a* ratio (5.8) from an Fe deficient coastal water, whereas, the same ratio was decreased to 1.3 after 2.5nM Fe addition. Wilken et al. [57] conducted a study on six diatom species and reported the formation of stronger frustules when cells are Fe limited. Takeda [20] reported that in an Antarctic diatom culture experiment, Fe limitation resulted in increased cellular silica content. Marchetti and Harison [58] conducted a laboratory experiment on six isolates of marine and coastal diatom P*seudo*-nitzschia and reported that under Fe deficient condition specific growth rate was decreased and silicate content per cell was increased. Our results are in agreement with these observations where lower growth rate and higher biogenic silica production was observed in the untreated controls (Fig. 8c).

Silicate concentrations in the ambient water also can affect BSi:Chl *a* ratios. However, for the present experiment, the added silicate levels were similar for all treatments and the observed change in BSi could therefore be attributed to Fe supply. The actual reason for enhanced Si contents in diatoms cells grown under low Fe concentration has been proposed to be an indirect one. The silicate uptake rate is not uniform throughout the cell cycle. But rather just before cell division in order to make the new frustules for the daughter cells, silicate uptake rates can be maximized [22]. Cells grown in low Fe therefore possess a prolonged silicate uptake stage as a lack of Fe leads to a delay in cell division resulting in high silicate content in the cells and slow growth rate [23]. On the contrary, cells grown in Fe enriched medium reduce Si:N uptake rate and can be because of higher nitrate uptake rate in presence of Fe compared to silicate. A number of recent investigations studying a variety diatom species and natural diatom communities revealed that higher Si:N content may result from increased silicate and decreased nitrate uptake rate under Fe deficient conditions [39]. It should be noted that in some diatoms, frustules silicification does not change in response to Fe stress, whereas, they show a difference in their cell morphometry by altering silica containing valve surface area relative to volume ratios [24]. For the present study, although BSi:Chl *a* ratios show a significant decrease in response to Fe enrichment, however, further information on Si:N uptake rates, cellular Si:N contents and cellular morphometry would be much more useful to confirm the observed trend.

5. Conclusions:

The present study revealed that *C. gracilis* is capable of growing under a wide range of Fe concentrations when exposed to high light by activating DD cycle. This particular ability of short term photo-acclimation might enable this diatom genus to be one of the most successful diatoms in the study area. Increase in Fe supply significantly decreases DT index and PP/LH pigment ratios and can be used as a physiological marker for Fe stress. Although, our preliminary observation indicates the possibility of reduced cellular silicate contents under Fe enriched conditions, however, additional information are needed to confirm the fact.

Acknowledgement: This study was conducted under the CSIR funding under the project OLP 1211. We would like to express our sincere gratitude to the Director, NIO for funding the study. We would like to thank the Scientists-In-charge, RC, Visakhapatnam and all of our colleagues and students from this center for their continuous support and encouragement. NIO contribution number for this manuscript is

References:

1. A. Butler, *Acquisition and utilization of transition metal ions by marine organisms,* Science. 281(1998), pp. 207 -210.
2. J. A. Raven, M. C. W. Evans, R. E. Korb, *The role of trace metals in photosynthetic electron transport in O_2 evolving organisms.* Photosynth. Res. 60(1999), pp. 111–149.
3. J. La Roche, R. J. Geider, L. M. Graziano, H. Murray, K. Lewis, *Induction of specific proteins in eukaryotic algae grown under iron-deficient, phosphorus-deficient, or nitrogen-deficient conditions,* J Phycol 29(1993), pp.767–777.
4. P. W. Boyd, et al., *Mesoscale iron enrichment experiments* 1993–2005, Synthesis and future directions, Science. 315 (2007), pp. 612–617.
5. E. V. Armbrust. The life of diatoms in the world's oceans. Nature. (2009) 459, pp. 185-192.
6. R. M. Greene, R. J. Geider, Z. Kobler, and P. G. Falkwoski, *Iron- induced changes in light harvesting and photochemical energy converson processe in Eukaryotic marine algae*, Plant Physiol. 100 (1992), pp. 565 -575.
7. J. La Roche, H. Murray, M. Orellana and J. Newton, *Flavodoxin expression as an indicator of iron limitation in marine diatoms,* J. Phycol. 31(1995), pp. 520 -530.
8. G. J. Doucette, and P. J. Harrison, *Some effects of iron and nitrogen stress on the red tide dinoflagellate Gymnodonium sanguineum*, Mar. Ecol. Progr. Ser. 62 (1990), pp. 293 -306.
9. G.J. Doucette, D.L. Erdner, M.L. Peleato, J.J. Hartman, and D.M. Anderson, *Quantitative analysis of iron-stress related proteins in Thalassia weissflogii: measurement of flavodoxin and ferredoxin using HPLC*, Mar. Ecol. Prog. Ser. 130(1996), pp. 269-276.
10. A. Kosakowska, J. Lewandowska, J. Ston, K. Burkiewicz, *Qualitative and quantitative composition of pigments in Phaeodactylum tricornutum (Bacillariophyceae) stressed by iron*, BioMetals; 17(2004), pp. 45 -52.
11. E. Boyle, 1998. *Pumping iron makes thinner diatoms*, Nature. 393, 733 -734.
12. M. Bertrand, *Carotenoides biosynthesis in diatoms*, Photosynth. Res. 106 (2010), pp. 89 -102.
13. F. Morales, A. Abadia, R. Belkhodja and J. Abadia, *Iron deficiency-induced changes in the photosynthetic pigment composition of field-grown pear (Pyrus communis L.) Leaves,* Plant Cell Environ. 17(1994), pp. 1153 -1160.
14. A. Hager, *The Reversible, Light-Induced Conversions of Xanthophylls in the Chloroplast*, in *Pigment in Plants*, eds. F. C. Czygan, Fisher, Stuttgart, 1980, 57–79.
15. M. Lohr, and C. Wilhelm, *Algae displaying diadinoxanthin cycle also possess the violaxanthin cycle,* Proc. Natl. Acad. Sci. 96(1999), pp. 8784 -8789.
16. W. Arsalane, B. Rousseau, and J. C. Duval, *Influence of the pool size of the xanthophyll cycle on the effects of light stress in a diatom: Competition between photoprotection and photoinhibition.* Photochem. Photobiol. 60 (1994), pp. 237–43.

17. M. Olaizola, and H. Y. Yamamoto*, Short-term response of the diadinoxanthin cycle and fluorescence yield to high irradiance in Chaetoceros muelleri (Bacillariophyceae).* J. Phycol. 30 (1994), pp. 606–12.

18. M. Laviale, and J. Neveux, Relationships between pigment ratios and growth irradiance in 11 marine phytopankton species, Mar. Ecol. Progr. Ser. 425(2011), pp. 63 -77.

19. D. A. Hutchins, and K.W. Bruland, *Iron-limited diatom growth and Si,N uptake ratios in a coastal upwelling regime*, Nature. 393(1998), pp. 561-564.

20. S. Takeda, *Influence of iron availability on nutrient consumption ratio of diatom iin oceanic waters*, Nature. 393 (1998), pp. 774 -777.

21. L. J. Hoffmann, I. Peeken, and K. Lochte, *Effects of iron on the elemental stoichiometry during EIFEX and in the diatoms Fragilariopsis kerguelensis and Chaetoceros dichaeta,* Biogeosci, 4(2007), pp. 569-579.

22. M. A. Brzezinski, *Cell cycle effects on the kinetics of silicis acis uptake and resource competiion amonf diatoms*, J. Plankton. Res. 14(1992), pp. 1511 -1539.

23. V. Martin-Jezequel, M. Hildebrand and A. Brzezinski, *Silicon metabolism in diatoms: Implications for growth*. J. Phycol. 36 (2000), pp. 821–840.

24. A. Marchetti and N. Cassar, *Diatom elemental and morphological changes in response to iron limitation: a brief review with paleoceanographic applications*, Geobiol. 7(2009), pp. 419-431.

25. S. Prasanna Kumar, J. Narvekar, M. Nuncio, A. Kumar, N. Ramaiah, S. Sardesai, M. Gauns, V. Fernandes, J. Paul, *Is the biological productivity in the Bay of Bengal light limited?* Current. Sci. 98(10) (2010), pp. 1331-1339.

26. J.T. Paul, N. Ramaiah, M. Gauns, V. Fernandes, *Predominance of few diatom species among highly diverse microphytoplankton assemblages in the Bay of Bengal*, Mar. Biol. 152(1) (2007), pp. 63 -75.

27. N. M. Price, G. Harrison, J. Hering, J. R. Hudson, P.M.V. Nirel, B. Palenick, and F. M. M. Morel, *Preparation and chemistry of the artificial algal culture medium Aquil,* Biol. Oceanogr. 6(1988/1989), pp. 443–461.

28. G. Rejomon, K. K. Balachandran. M. Nair, T. Joseph. P. K. Dineshkumar, C. T. Achuthankutty, K. K. C Nair, N. G. K. Pillai, *Trace metal concentrations in zooplankton from the eastern Arabian Sea and western Bay of Bengal,* Environ Forensics. 9(2008), pp. 22-32.

29. G. Rejomon, P.K. Dinesh Kumar, M. Nair K. R. Muraleedharan, *Trace metal dynamics in zooplankton from the Bay of Bengal during summer monsoon,* Environ. Toxicol. 25(6) (2010), pp. 622-633.

30. R.F. Nolting, L.J.A. Gerringa, M.J.W. Swagerman, K.R. Timmermans, H.J.W. de Baar., *Fe (III) speciation in the high nutrient, low chlorophyll Pacific region of the Southern Ocean,* Mar Chem. 62(1998)., pp.335-352.

31. R. Suzuki, and T. Ishimaru, *An improved method for the determination of phytoplankton chlorophyll using N,N-dimethylformamide.* J. Oceanogr. 46 (1990), pp. 190–194.

32. E. Paasche, *Silicon and Ecology and Marine planktonic diato. 1. Thalassiosira pseudonana (Cyclotella nana) grown in chemostats with silicate as the limiting nutrient,* Mar. Biol. 19(1973), pp.117 -126.
33. J. D. Strickland, and T. R. Parsons, *A practical handbook of Seawater analysis*. Bulletin of Fisheries Research Board of Canada, Canada (1972).
34. L.V. Heukelem, and C.S. Thomas, *Computer- assisted high-performance liquid chromatography method development with applications to the isolation and analysis of phytoplankton pigments*, J. Chromatogr. 910 (1) (2001), pp. 31 – 49.
35. J. A. Guikema, and L. A. Sherman, *Organization and function of chlorophyll in membranes of cyanobacteria during iron starvation*, Plant. Physiol. 73 (1983), pp. 1061 -1082.
36. R. M. Greene, R. J. Geider, and P. G. Falkowski, *Effect of iron limitation on photosynthesis in a marine diatom*, Limnol. Oceanogr. 36 (1991), pp. 1772 – 1782.
37. S. C. Spiller, A. M. Castelfranco, P. A. Castelfranco, *Effects if iron and oxygen on chlorophyll biosynthesis. I. In vivo observation on iron and oxygen deficient plants.* Plant Physiol. 69(1982), pp. 107 -111.
38. M. H. Yu, and G. W. Miller, *Formation of δ-aminolevulinic acid in etiolated and iron stressed barley,* J. Plant Nutr. 5 (1982), pp. 1259 -1271.
39. K. R. Timmermans, W. Stolte, H. J. W. Debaar, *Iron-mediated effects on nitrate reductase in marine phytoplankton,.* Mar. Biol. 121(1994), pp. 389–396.
40. J. H. Martin, K. H. Coale, K. S. Johnson, et al., *Testing the iron hypothesis in ecosystems of the equatorial Pacific Ocean,* Nature. 371(1994), pp. 123 -129.
41. A. Marchetti, et al., *Comparative metatranscriptomics identifies molecular bases for the physiological responses of phytoplankton to varying iron avai*lability, Proc. Natl. Acad. Sci. USA. 109 (6) (2012), pp. 317-325.
42. S. W. Jeffrey, and M. Vesk, *Introduction to marine phytoplankton and their pigment signatures,* in: Phytoplankton pigment in oceanography, S. W. Jeffrey, R. F. C. Mantoura and S. W. Wright, eds., UNESCO Publishing, (1997) pp. 37 -84
43. J. M. Escoubas, M. Lomas, J. La Roche, and P. G. Falkwoski, *Light intensity regulation of cab gene transcription is signaled by the redox state of plastoquinone pool*, Proc. Nat. Acad. Sci. USA. 92(1995), pp. 10237 -10241.
44. A. Mortain-bertrand, J. Bennett and P.J. Falkowski, *Photoregulation of the light harvesting chlorophyll protein complex associated with photosystem II in Dunaliella salina,* Plant. physiol. 94(1990), pp. 304 – 311.
45. A. Beer, M. Juhas and C. Buechel, *Influence of different light intensities and different iron nutrition to the photosynthetic apparatus in the diatom cyclotella meneghiniana (Bacillariophyceae)*, J. Phycol. 47(2011), pp. 1266–1273.
46. M. Davey, and R. J Geider, *Impact of iron limitation on the photosynthetic apparatus of the diatom Chaetoceros Muelleri (Bascillariophyceae)*, J. Phycol. 37(2001), pp. 987 -1000.

47. T. V. Oijen, M. A. V Leeuwe, W. W. C. Gieskes and H. J. W. de Baar, *Effects ofrion limitation on photosynthesis and carbohydrate metabolism in the Antartic diatom Chaetoceros brevis (Bacilariophyceae),* Eur. J. Phycol. 39(2004), pp. 161 -171.

48. Y. Kashino and S.Kudoh*, Concerted response of xanthophyll-cycle pigments in a marine diatom Chaetoceros gracilis to shift in light condition*, J. Phycol. 51(3) (2003), pp.168 -172.

49. M. Lohr, and C. Wilhelm, *Xanthophyll synthesis in diatoms: quantification of putative intermediates and comparison of pigments conversion Kinetics rate constant derived from a model*, Planta. 212(2001), pp. 382 -391.

50. J. Lavaud, B, Rousseau, H. J. van Gorkum and A. L. Etienne, *Influence of the diadinoxanthin pool size on photoprotection in the marine planctonic diatom Phaeodactylum tricornutum,* Plant Physiol. 129(2002), pp.1398–406.

51. M. Juhas, and C. Buechel, *Properties of photosystem I antenna protein complexes of the diatom cyclotella meneghiniana,* J. Exp. Bot. doi.10.1093/jxb/ers049 (2012).

52. R. Goericke and N. A. Welschmeyer, *Pigment turnover in tge marine diatom Thalassiosira weissflogii II. The $^{14}CO_2$-labelling kinetics of carotenoids*, J. Phycol 28 (1992), pp. 507 -517.

53. T. Fujiki and S. Taguchi, *Relationship between light absorption and the xanthophyll-cycle pigments in marine diatoms*, Plankton. Biol. Ecol. 48(2) (2001), pp. 96 -103.

54. W. H. Van De Poll, P. J. Janknegt, M. A. Van Leeuwe, R. J. W. Visser, , A. G. J. Buma, *Excessive irradiance and antioxidant response of an Antarctic marine diatom exposed to iron limitation and to dynamic irradiance,* J. Photochem. Photobiol. B Biol. 94 (2009), pp. 32–37.

55. Y. Ikeda, M. Komura, M. Watanabe, C. Minami, H. Koike, S. Itoh, Y. Kashino, K. Satoh, *Photosystem I complexes associated with fucoxanthin-chlorophyll-binding protein from a marine centric diatom Chaetoceros gracilis*, Biochim Biophys Acta 1777(2008), pp. 351 -361.

56. C. Dimier, F. Corato, F. Tramontano, and C. Brunet, *Photoprotection and xanthophyll-cycle activity in three marine diatoms*, J. Phycol. 43(2007), pp, 937 -947.

57. S. Wilken, W. Rubner, B. Hoffmann., L. Hoffmann, J.N. Hersch, R. Merkel, N. Kirchgessner, I. Peeken and S. Dieluweit, *Diatom frustules show increased mechanical strength and altered valve morphology under iron limitation*, Limnol. Oceanogr. 56(4) (2011), pp. 1399 -1410.

58. A. Marchetti and P. J. Harrison, *Coupled changes in the cell morphology and the elemental (C, N, and Si) composition of the pennate diatom Pseudo-nitzschia due to iron deficiency*. Limnol. Oceanogr. 52(5) (2007), pp. 2270–2284.

Table 1: Concentrations of Chl *a*, BSi and BSi:Chl *a* ratios in response to different iron levels derived from individual experiments (The average values with standard deviations are given in the last part of the table and the values were averaged from the individual experiments).

Dates	Added Fe level (nM)	Chl *a* (μg L^{-1})	BSi (μM)	Bsi:Chl*a*	Silicate uptake (μM)
5/11/2011	Control -1	7.90	12.67	1.60	-
	Control -2	6.12	10.34	1.69	-
	200	113.86	34.27	0.30	-
	200	128.15	44.70	0.35	-
	200	111.80	43.20	0.39	-
	200	109.96	45.80	0.42	-
8/11/2011	Control	7.20	-	-	-
	200	134.64	-	-	-
	400	122.40	-	-	-
	600	113.21	-	-	-
	800	117.30	-	-	-
	1000	114.11	-	-	-
	1200	118.31	-	-	-
	1400	106.24	-	-	-
	1600	101.19	-	-	-
	1800	102.16	-	-	-
	2000	100.72	-	-	-
18/11/2011	Control	6.40	7.25	1.13	8.53
	25	9.57	7.31	0.76	12.61
	40	17.01	14.77	0.87	15.40
	50	34.67	20.15	0.58	29.29
	70	46.91	25.94	0.55	35.11

	60	72.56	37.54	0.52	40.66
	80	98.58	55.61	0.53	61.12
	200	113.40	51.20	0.45	56.32
23/11/2011	Control	7.66	8.56	1.12	9.84
	25	17.58	9.11	0.52	11.75
	50	44.50	22.63	0.51	19.95
	100	105.36	21.62	0.22	25.60
	150	113.63	32.75	0.29	34.12
	200	106.51	39.74	0.37	36.53
	250	102.49	38.55	0.38	40.89
	300	124.84	46.37	0.37	44.78
	500	104.77	34.59	0.33	36.78
	1000	114.93	42.41	0.37	42.18
Average	Control (n =5)	7.06±0.9	7.90±0.93	1.32±0.33	9.19±0.92
	25 (n=2)	13.57±5.7	8.21±1.27	0.64±0.17	12.18±0.60
	50 (n=2)	39.58±7.0	21.39±5.56	0.54±0.25	24.62±6.61
	200 (n =7)	116.90±10.4	43.15±5.74	0.38±0.06	46.42±14
	1000 (n =2)	114.52±0.58	-	-	-

Table 2: Pigment ratios derived from individual experiment in response to different iron concentrations over the experimental range. The last two columns represent average ± SD values for the control and 200nM Fe treatments.

Date	Added Fe Level (nM)	Fuco/Chl *a*	Chl *c*/Chl *a*	β-Caro /Chl *a*	DD/β-Caro	DD/Chl *a*	DT/Chl *a*	DT/(DT+DD)	PP/LH
5/11/2011	Control -1	0.35	0.090	0.080	2.28	0.18	0.163	0.47	0.29
	Control -2	0.38	0.064	0.078	2.54	0.20	0.193	0.49	0.32
	200	0.33	0.080	0.093	1.53	0.14	0.029	0.17	0.19
	200	0.30	0.072	0.091	1.36	0.12	0.019	0.14	0.17
	200	0.43	0.097	0.106	1.39	0.15	0.022	0.13	0.18
	200	0.40	0.078	0.101	1.64	0.17	0.041	0.20	0.21
23/11/2011	Control	0.37	0.079	0.079	2.39	0.19	0.175	0.48	0.31
	25	0.31	0.051	0.090	1.68	0.15	0.164	0.52	0.30
	50	0.35	0.058	0.091	1.56	0.14	0.075	0.35	0.22
	100	0.34	0.059	0.088	1.50	0.13	0.050	0.27	0.19
	150	0.33	0.070	0.095	1.76	0.17	0.051	0.23	0.22
	200	0.27	0.063	0.084	1.80	0.15	0.043	0.22	0.21
	300	0.30	0.074	0.092	1.67	0.15	0.039	0.20	0.21
	500	0.32	0.073	0.098	1.82	0.18	0.045	0.20	0.23
	1000	0.34	0.077	0.091	1.58	0.14	0.020	0.12	0.18
Average	Control (n =3)	0.37±0.015	0.078±0.013	0.079±0.001	2.40±0.13	0.19±0.01	0.18±0.02	0.48±0.01	0.31±0.02
	200 (n =5)	0.35±0.067	0.078±0.013	0.095±0.009	1.54±0.18	0.15±0.02	0.031±0.01	0.17±0.04	0.19±0.02

Table 3: Paired t-test results showing t- values, degree of freedom (df) and probability (P) levels for different pigment contents, their ratios, biogenic silica and biogenic silica to Chl *a* ratios (the results show the significance of difference between control (no added iron) and iron treated samples).

	t	df	Response	P
Fuco/Chl *a*	2.15	13	NSC	<0.1
Chl *c*/Chl *a*	0.83	13	NSC	>0.1
β-carotene/Chl *a*	-8.45	13	Increased	<0.001
DD/β-carotene	9.37	13	Decreased	<0.001
DD/Chl *a*	6.22	13	Decreased	<0.001
DT/Chl *a*	9.19	13	Decreased	<0.001
DT/(DT+DD)	8.08	13	Decreased	<0.001
PP/LH	7.78	13	Decreased	<0.001
Chl *a* ($\mu g\ L^{-1}$)	-42.59	33	Increased	<0.001
BSi ($\mu mol\ L^{-1}$)	7.45	22	Increased	<0.001
BSi:Chl *a*	8.32	22	Decreased	<0.001

Table 4: Regression analysis results showing R^2 values, sample size (n) , Probability (P) levels and type of responses (positive, negative or insignificant) to different iron concentrations over the experimental range.

Parameters	R^2	n	P	Response
Chl *a* (Fluorometric analysis)	0.724	35	<0.001	Positive
Chl *a* based specific growth rate	0.793	35	<0.001	Positive
Chl *a* (HPLC analysis)	0.836	16	<0.001	Positive
Fuco	0.850	15	<0.850	Positive
Fuco/Chl *a*	0.069	15	>0.1	Insignificant
Chl *c*	0.856	15	<0.856	Positive
Chl *c* /Chl *a*	0.006	15	>0.1	Insignificant
Fuco/Chl *c*	0.123	15	>0.1	Insignificant
DD	0.794	15	<0.001	Positive
DD/Chl *a*	0.353	15	>0.1	Insignificant
DT	0.303	15	>0.1	Insignificant
DT/Chl *a*	0.826	15	<0.001	Negative
β	0.848	15	<0.001	Positive
β/Chl *a*	0.104	15	>0.1	Insignificant
DT/(DT+DD)	0.854	15	<0.001	Insignificant
DD/β	0.609	15	<0.02	Negative
BSi	0.637	20	<0.001	Positive
BSi:Chl *a*	0.744	20	<0.001	Negative
BSi:Fuco	0.767	13	<0.001	Negative

Legends to Figures:

Fig. 1: Map showing the sampling site.

Fig. 2: a) Light intensity over 12:12 hrs light : dark cycle during the pre-culture and experimental periods (average ±SD); b) total chlorophyll concentrations measured by fluorometry in relation to different iron levels; c) chlorophyll *a* (derived from fluorometric method) based specific growth rates in relation to different iron concentrations.

Fig. 3: HPLC chromatogram depicting individual peak of cellular pigments (Chl *a*, Chl *c*, Fuco, DD, DT and *β*-carotene) from the a) untreated control (b) 25nM (c) 50nM (d) 100nM (e) 150nM and (f) 500nM Fe treatments.

Fig. 4: a) Fuco and b) Chl *c* concentrations in relation to different iron levels; c) Fuco/Chl *a* ratios d) Chl *c*/ Chl *a* ratios and e) Fuco/ Chl ratios in relation to different iron concentrations.

Fig. 5: Concentrations of a) DD b) DT and c) *β*-carotene in relation to iron levels; the ratios of d) DT/ Chl *a*, e) DT/Chl *a* and f) *β*-carotene/Chl *a* over the experimental iron range.

Fig. 6: Total pool of a) LH pigments b) PP pigments and c) ratios of PP/LH pigments in relation to iron levels

Fig. 7: a) DT index [DT/(DT+DD)] and b) the ratios of DD/*β*-carotene in relation to different iron levels.

Fig. 8: a) cellular BSi contents b) relation between BSi and Chlorophyll *a* and c) ratios of BSi:Chl *a* in relation to different iron levels.

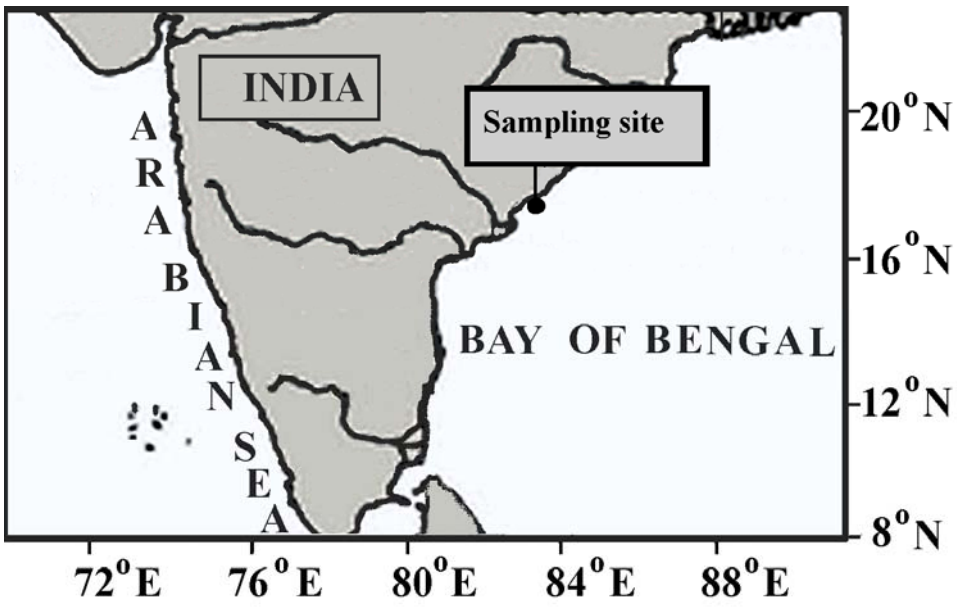
INDIA
Sampling site
ARABIAN SEA
BAY OF BENGAL
20°N
16°N
12°N
8°N
72°E
76°E
80°E
84°E
88°E

Fig. 1

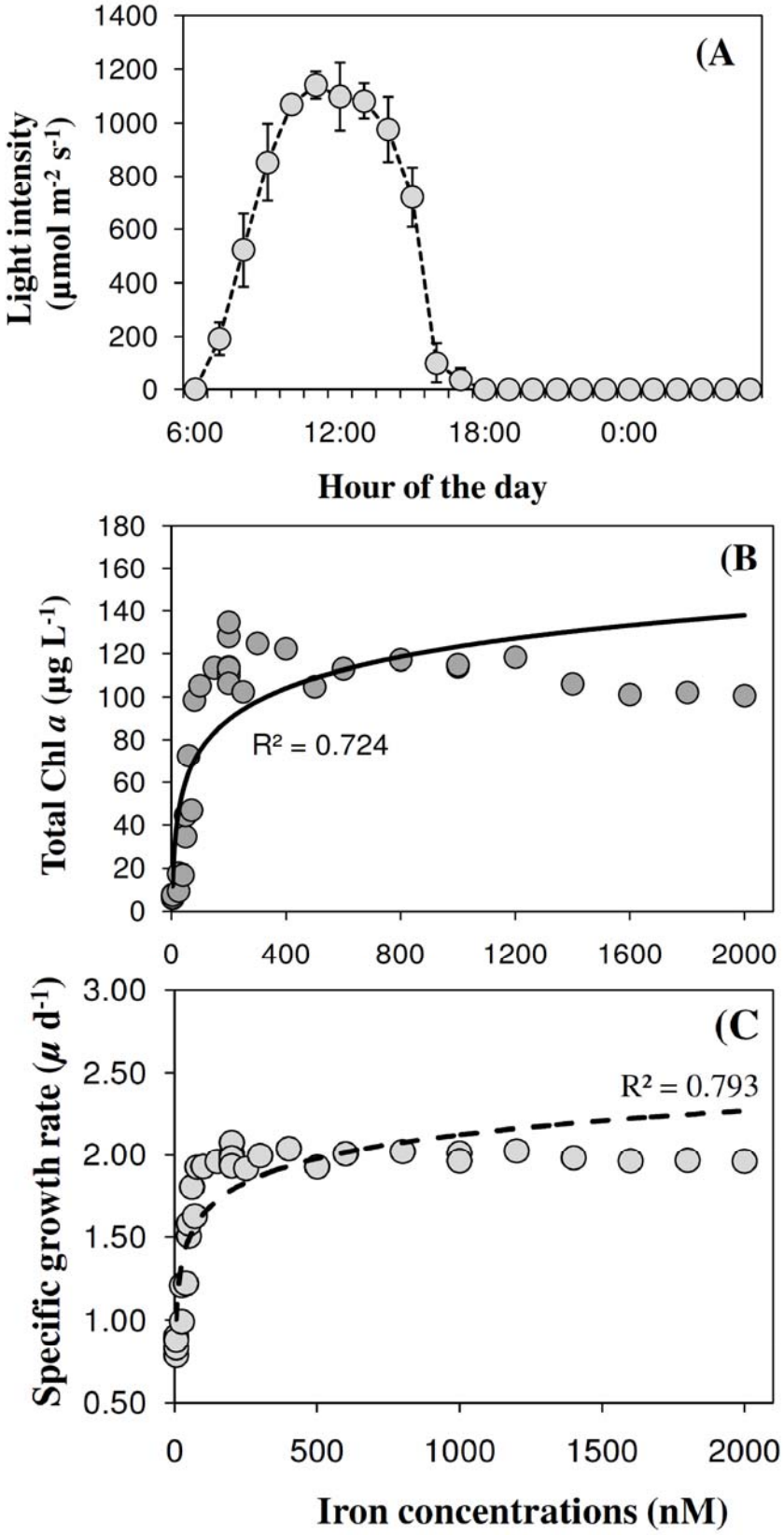
(A
Light intensity (µmol m-2 s-1)
1400
1200
1000
800
600
400
200
0
6:00
12:00
18:00
0:00
Hour of the day
(B
Total Chl a (µg L-1)
180
160
140
120
100
80
60
40
20
0
R² = 0.724
0
400
800
1200
1600
2000
(C
Specific growth rate (µ d-1)
3.00
2.50
2.00
1.50
1.00
0.50
R² = 0.793
0
500
1000
1500
2000
Iron concentrations (nM)

Fig. 2

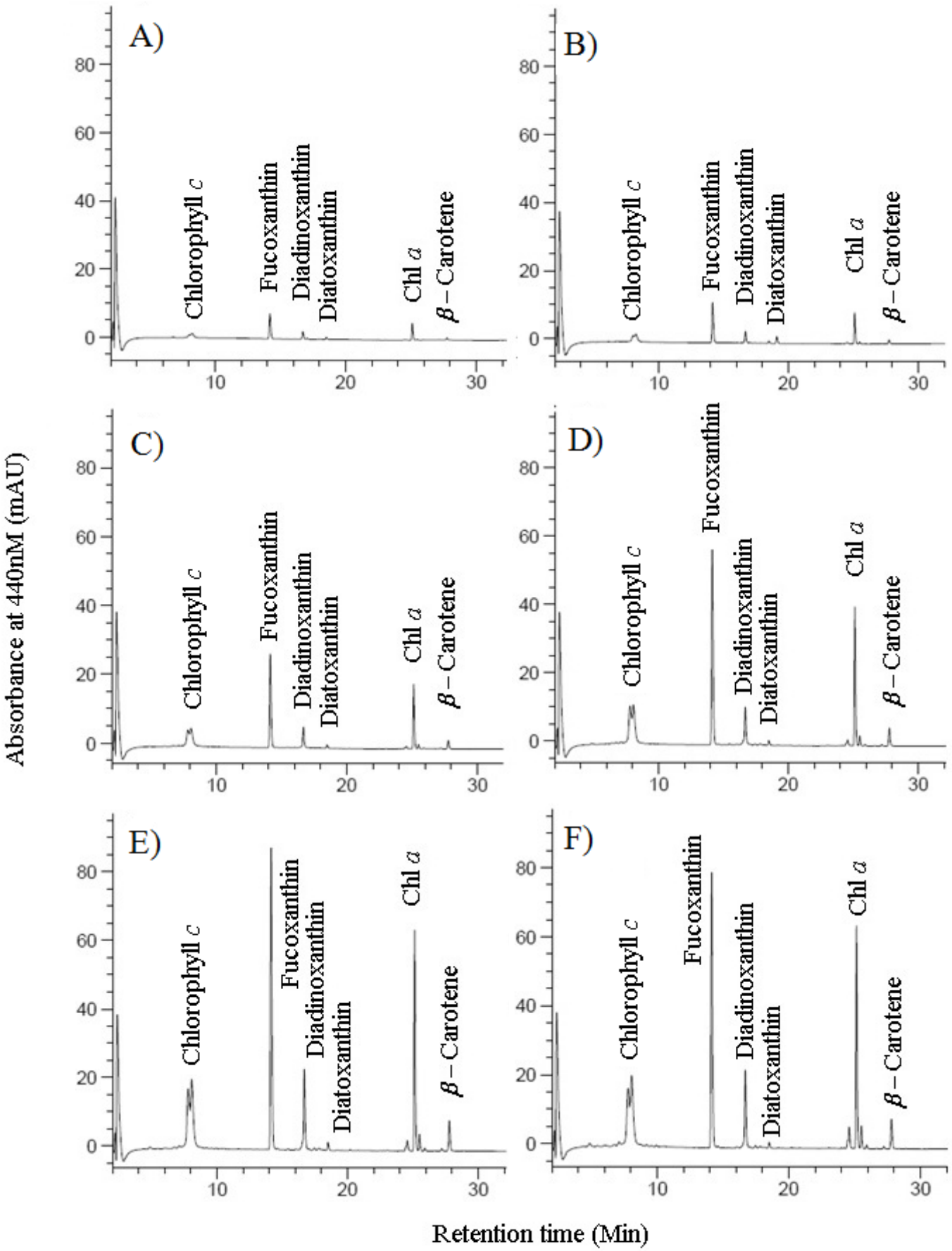
A)
B)
C)
D)
E)
F)
Chlorophyll c
Fucoxanthin
Diadinoxanthin
Diatoxanthin
Chl a
β – Carotene
Absorbance at 440nM (mAU)
Retention time (Min)

Fig. 3

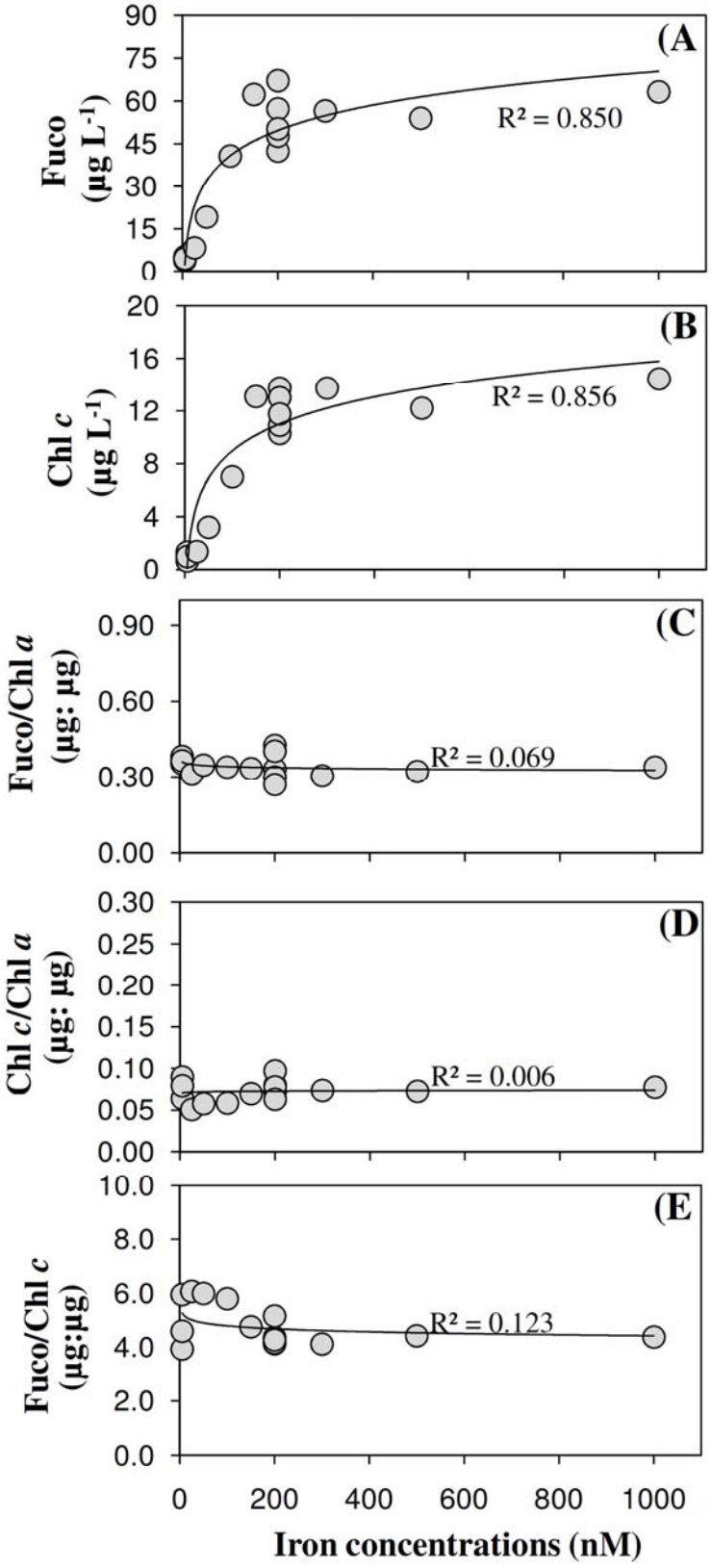
(A)
Fuco (µg L-1)
R² = 0.850
(B)
Chl c (µg L-1)
R² = 0.856
(C)
Fuco/Chl a (µg: µg)
R² = 0.069
(D)
Chl c/Chl a (µg: µg)
R² = 0.006
(E)
Fuco/Chl c (µg:µg)
R² = 0.123
Iron concentrations (nM)

Fig. 4

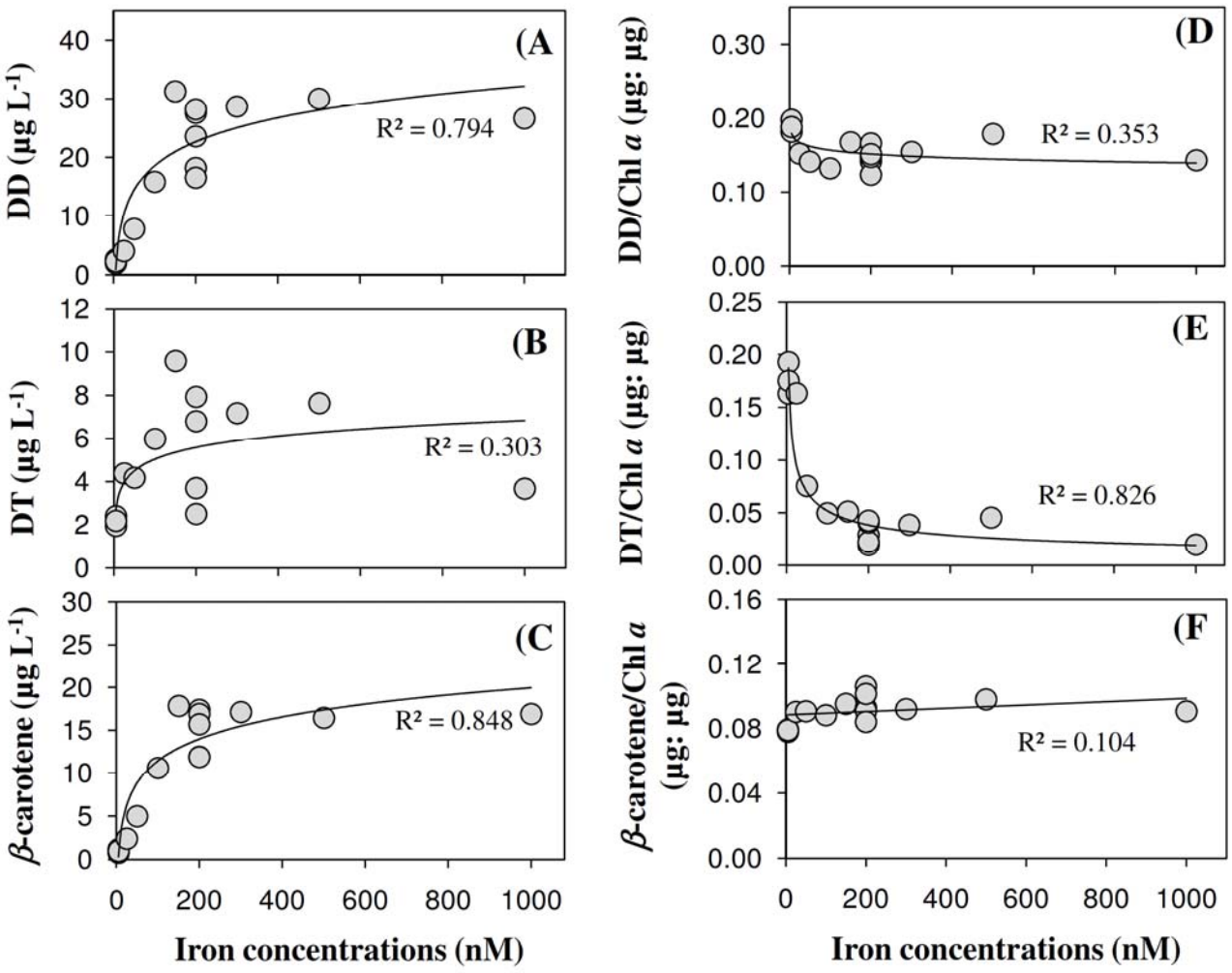
(A)
DD (µg L-1)
R² = 0.794
(B)
DT (µg L-1)
R² = 0.303
(C)
β-carotene (µg L-1)
R² = 0.848
Iron concentrations (nM)
(D)
DD/Chl a (µg: µg)
R² = 0.353
(E)
DT/Chl a (µg: µg)
R² = 0.826
(F)
β-carotene/Chl a (µg: µg)
R² = 0.104
Iron concentrations (nM)

Fig. 5

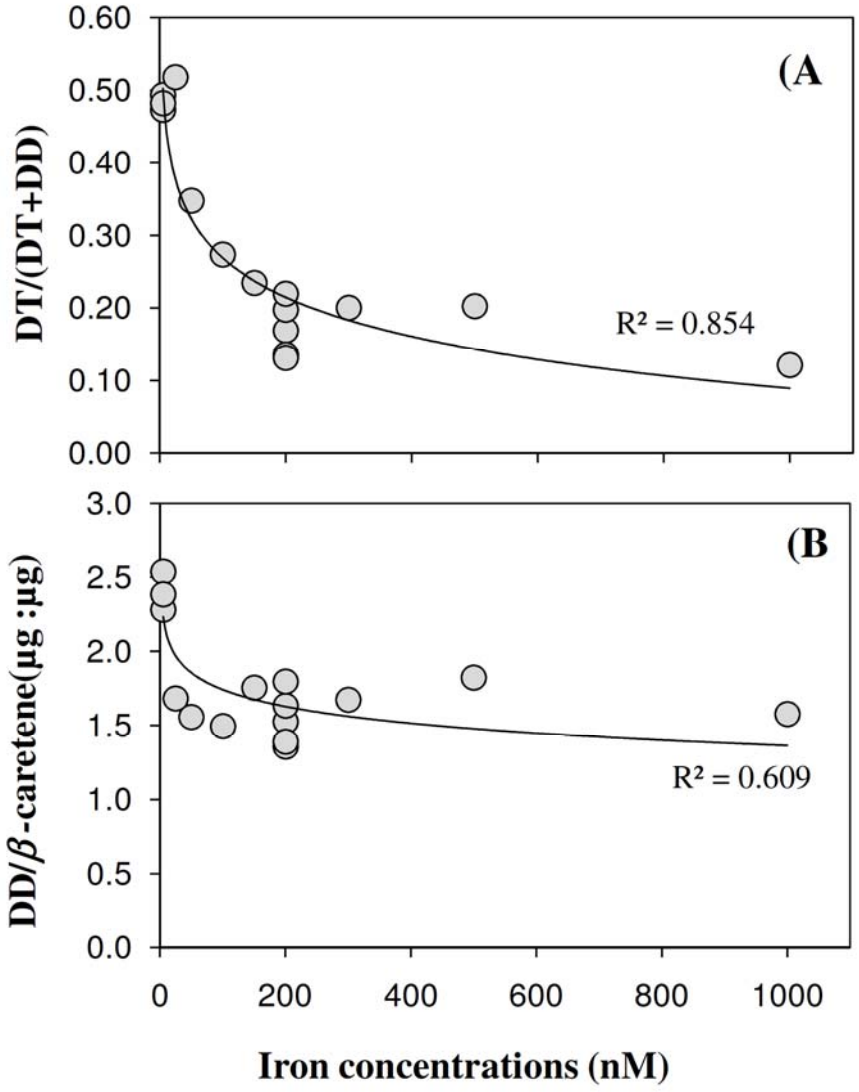
(A
DT/(DT+DD)
0.60
0.50
0.40
0.30
0.20
0.10
0.00
R² = 0.854
(B
DD/β-caretene(µg :µg)
3.0
2.5
2.0
1.5
1.0
0.5
0.0
R² = 0.609
0
200
400
600
800
1000
Iron concentrations (nM)

Fig. 6

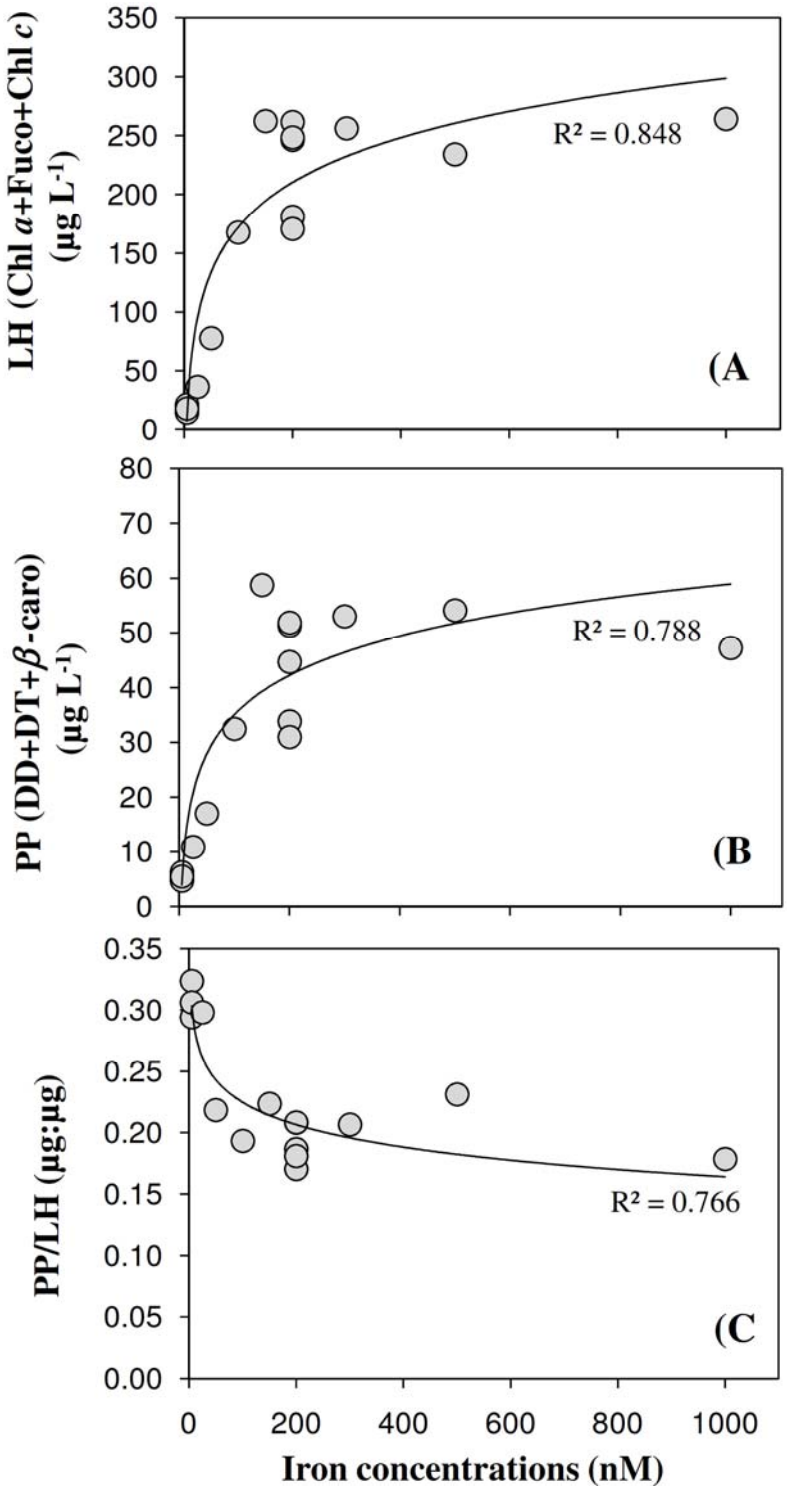
LH (Chl a+Fuco+Chl c) (µg L-1)
PP (DD+DT+β-caro) (µg L-1)
PP/LH (µg:µg)
R² = 0.848
R² = 0.788
R² = 0.766
(A
(B
(C
Iron concentrations (nM)

Fig. 7

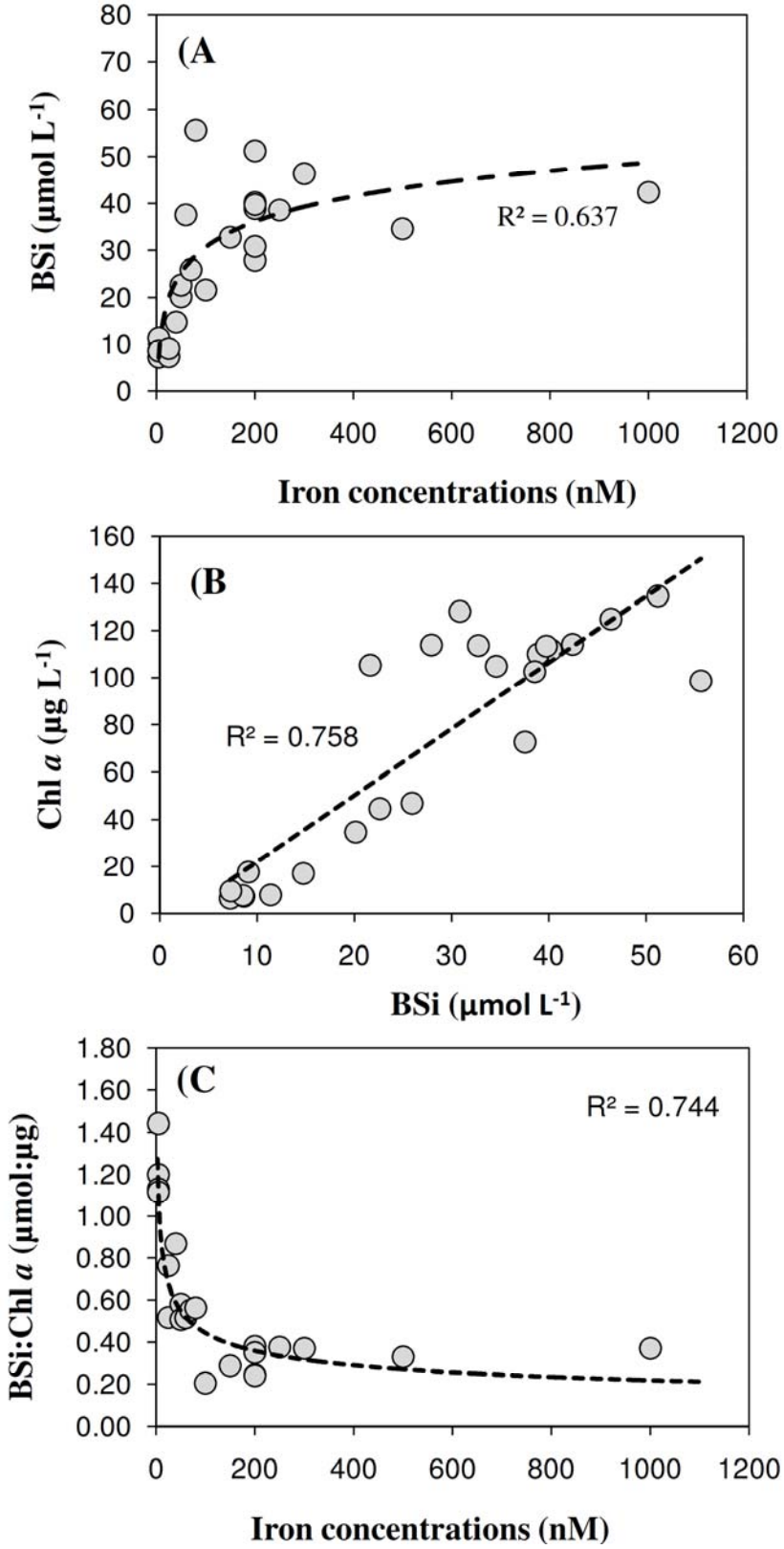
(A)
BSi (µmol L-1)
R² = 0.637
Iron concentrations (nM)
(B)
Chl a (µg L-1)
R² = 0.758
BSi (µmol L-1)
(C)
BSi:Chl a (µmol:µg)
R² = 0.744
Iron concentrations (nM)

Fig. 8